J Supercond Nov Magn (2012) 25:2389–2393
DOI 10.1007/s10948-012-1613-2

ORIGINAL PAPER

Low Field Microwave Absorption in Nanostructured Ferrite Ceramics Consolidated by Spark Plasma Sintering

R. Valenzuela · S. Ammar · S. Nowak · G. Vazquez

Received: 27 April 2012 / Accepted: 6 May 2012 / Published online: 17 May 2012

Abstract The low field microwave absorption (LFMA at 9.5 GHz) properties of clusters of $Zn_{0.5}Ni_{0.5}Fe_2O_4$ ferrite nanoparticles (NPs) consolidated by spark plasma sintering (PSP at temperatures in the 350–500 °C range) are analyzed. LFMA measurements were carried out at 77 and 300 K. The clusters, formed by ∼6 nm NPs, were first obtained by the forced hydrolysis in a polyol method from the corresponding metal acetates. It is found that the sign of LFMA, associated with the spin arrangement in the ferrite depends on the degree of consolidation. For monodispersed NPs, no change of sign is observed at low temperatures. For the as-produced clusters and the consolidated samples, a progressive change in the sign of the signal is observed as the sintering temperature is increased. This change of sign is associated with the occurrence of the triangular or canted Yafet–Kittel spin arrangement.

Keywords Microwave absorption · Ferromagnetic resonance · Magnetic nanoparticles · Ferrites

1 Introduction

Magnetic nanoparticles present an additional complexity as compared with other materials when their dimensions are reduced to the nanometric scale. In addition to the effects of surface, due to the fact that the ratio of surface atoms to core atoms becomes significant, several critical parameters concerning the magnetic structure and phenomena are found in the same 1–100 nm size range. Among such critical parameters in magnetism, we can mention, for instance, the change from multi to single domain structure, the exchange correlation length, and the critical size for superparamagnetic behavior. Also, nanoparticles can have strong mutual interactions by dipolar, or exchange mechanisms.

Microwave absorption by materials can have a resonance nature, but recently a non-resonant phenomenon occurring at magnetic fields significantly lower than the ferromagnetic resonance field has also been reported in a wide variety of magnetic materials such as amorphous ribbons [1–3], glass-coated microwires [4–6], amorphous thin films [7], multilayers [8], bulk ferrites [9, 10], ferrite nanoparticles [11], manganites [12, 13], and small band gap insulators [14].

The forced hydrolysis in a polyol method to synthesize magnetic nanoparticles is a very fast and convenient method, allowing the preparation of nanoparticles (NPs) as small as 5 nm [15, 16]. In this method, the acetates of the involved metals are dissolved in a polyol, typically diethylene glycol, brought at a rapid heating rate to boiling, and maintained in reflux for 2–3 hours. NPs precipitated and are recuperated by centrifugation. By varying the synthesis parameters, some variations in NPs size and aggregation state can be tailored.

For many applications of nanostructured magnetic materials, especially in electronics, solid bodies are needed. These can be obtained by powder sintering; however, classic sintering techniques are carried out at high temperatures, which promote grain growth and, therefore, the loss of the small size-related novel properties. A recently developed technique, spark plasma sintering (SPS) [17, 18], can effectively consolidate powders into solid bodies maintaining the

R. Valenzuela (✉) · G. Vazquez
Departamento de Materiales Metálicos y Cerámicos, Instituto de Investigaciones de Materiales, Universidad Nacional Autónoma de México, AP 70-360, C.P. 04510, México D.F., México
e-mail: monjaras@unam.mx

S. Ammar · S. Nowak
ITODYS, UMR-CNRS 7086, Université de Paris-Diderot, 75205 Paris cedex, France

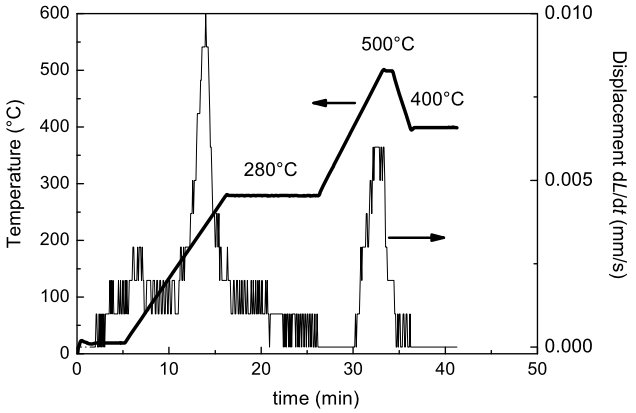

Fig. 1 Typical plot from an SPS experiment; temperature and derivative of distance between pushing rods as a function of time

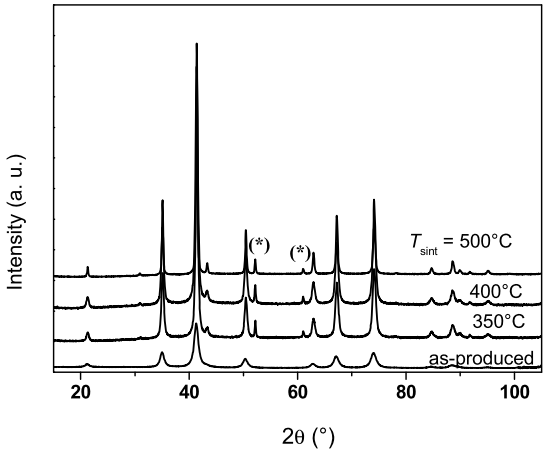

Fig. 2 X-ray diffraction of all the samples, for the different sintering temperatures

small (nanometric) grain size. In this technique, powders are pressed in a graphite mould which is also subjected to large electrical pulses. SPS allows very fast heating (and cooling) rates, as well as unusually low sintering temperatures.

In this paper, we have combined NPs synthesized by the polyol technique with a subsequent SPS sintering. The use of initial nanometric powders should allow extremely low sintering temperatures for very short times, therefore, maintaining the grain size within the nanometric range. The microwave absorption properties of these samples are then studied.

2 Experimental Procedure

Ferrite nanoparticles (NPs) of composition $Zn_{0.5}Ni_{0.5}Fe_2O_4$ were prepared by forced hydrolysis in a polyol [15, 16] from the corresponding iron, nickel, and zinc acetates. We used synthesis conditions (gently stirring and boiling) which allowed obtaining clusters of about 22 nm in size with an average crystal size also of ∼5 nm, with an epitaxial character for the second. The comparison of low field microwave absorption (LFMA) between monodispersed and clustered nanoparticles has been presented elsewhere [11]. The obtained dark brown powders were recovered by centrifugation, washed in ethanol, and finally dried at 50 °C in air. Clustered powders were subsequently consolidated by the spark plasma sintering (SPS) method, at temperatures of 350–500 °C, under a pressure of 100 MPa, for periods of time between 5 and 10 min. A typical SPS process is shown in Fig. 1. Several parameters can be plotted as a function of time. In this figure, we show the temperature and the derivative, dL/dt, of the reduction in the distance between the pushing rods in the graphite crucible. This parameter displays therefore an indication of the reduction in volume of the sample during the process, which is directly related with the sintering process.

The X-ray diffraction pattern of samples was obtained in a Panalytical XperPro diffractometer equipped with a multichannel detector (X'celerator), using Co K_α radiation. High-resolution transmission electron microscopy (HRTEM) observation was performed by means of a JEOL 100-CX transmission electron microscope operating at 100 kV. A JEOL JES-RES 3X Spectrometer was used for the microwave absorption measurements, operating in the X-band (8.8–9.8 GHz) at room temperature (300 K), and at liquid nitrogen point (77 K). For the low field measurements, any remanence in the electromagnet was digitally compensated by a JEOL ES-ZCS2 Zero-Cross Sweep unit, allowing measurements to be performed accurately by cycling the DC magnetic field to +1000 Oe and −1000 Oe about zero.

3 Results and Discussion

The XRD patterns, Fig. 2, showed a single spinel phase for all the thermal treatments, except for a small peak corresponding to metallic nickel (indicated by an asterisk in Fig. 2).

Due to the reduction conditions during SPS process, where the powder is contained in graphite film and a high-vacuum chamber, a small quantity of some cations can be reduced to the metallic state. The observed concentration, indicated by the size of the diffraction peaks is, however, quite small.

Scanning and high resolution transmission electron microscopy (SEM and HRTEM, respectively) confirmed that SPS can achieve a consolidated, high density body with limited grain growth, thanks to a very rapid process at low temperatures, as appears in Fig. 3, where the sample sintered at the highest temperature (500 °C) is shown.

We turn now to LFMA results, Fig. 4. The graphs at the left (Figs. 4a, 4b, and 4c) present the measurements carried

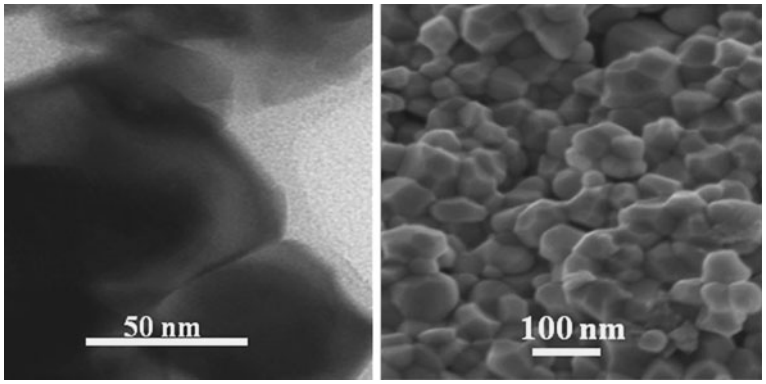

Fig. 3 HRTEM (*left*) and SEM (*right*) micrographs of the sample sintered at 500 °C

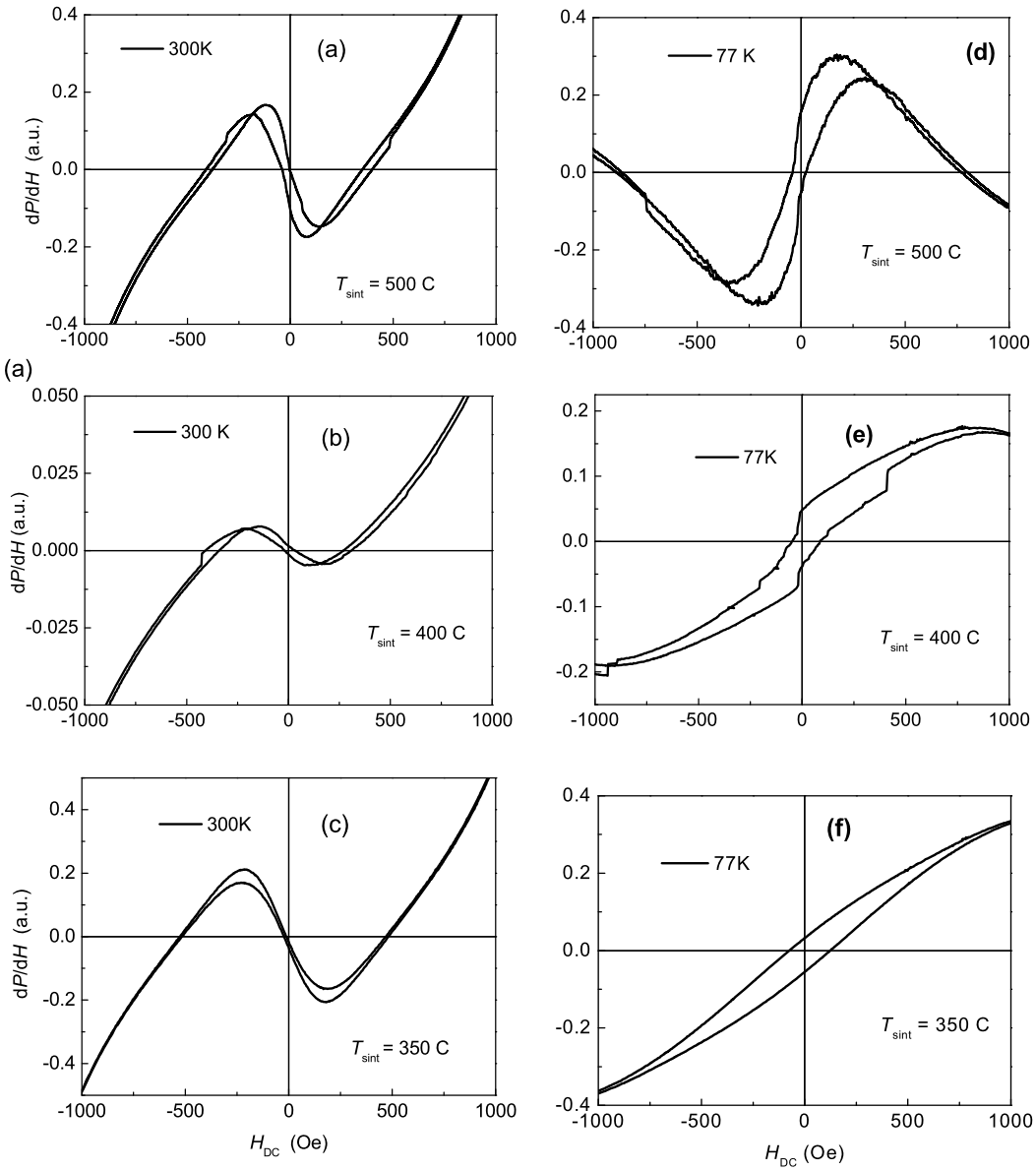

Fig. 4 LFMA samples: (**a**) and (**d**) sintered at 500 °C, (**b**) and (**e**) sintered at 400 °C, and (**c**) and (**f**) at sintered at 350 °C. Measurement temperature was 300 K (*left*) and 77 K (*right*)

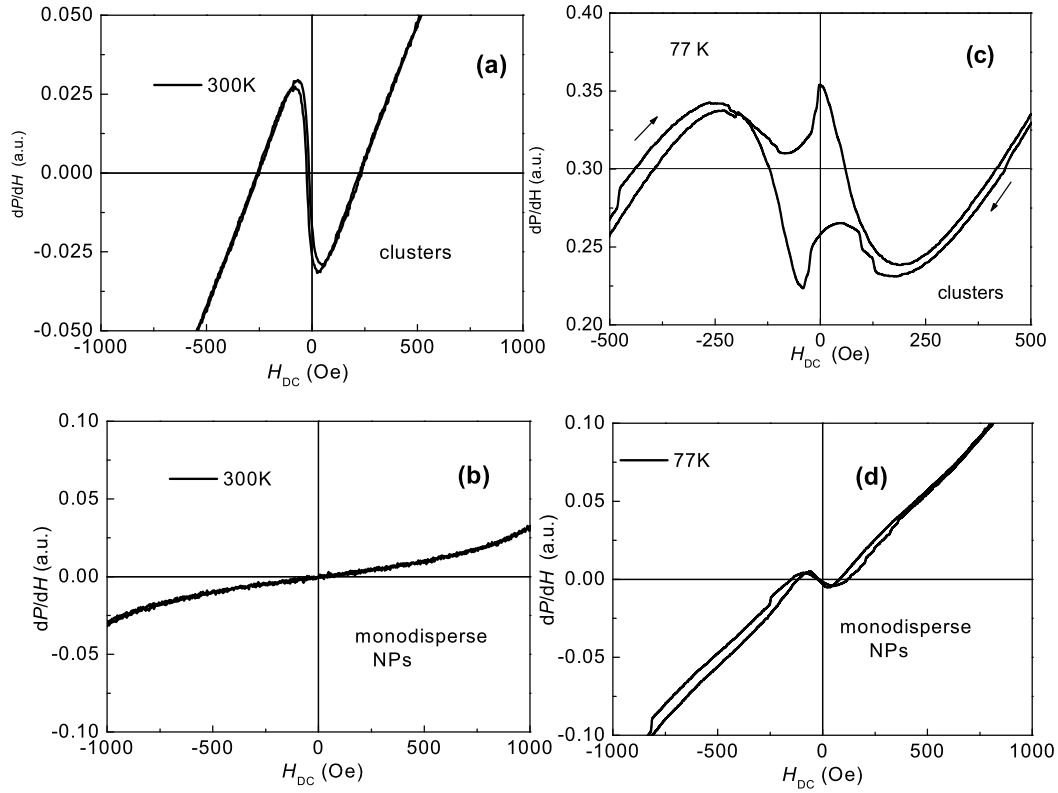

Fig. 5 LFMA measurements in as-produced NPs in two aggregation states: clusters (*high part*) and monodisperse NPs (*lower section*). Measurement temperature: 300 K at *left*, 77 K at *right*

out at room temperature for samples sintered by SPS at 500, 400, and 350 °C, respectively. They show the same general shape, i.e., a maximum for negative fields and a minimum for positive magnetic fields, with just small changes in the amplitude and the magnetic field corresponding to the maximum and the minimum. We can call this microwave absorption signal the "positive" signal as it has the same shape than the signal observed in ferromagnetic and paramagnetic resonance experiments.

It has been shown [2, 6] that the separation between peaks (which can be known as $2\Delta H_K$) is directly associated with the total anisotropy field of the sample. A decrease in H_K (as observed from Fig. 4a to Fig. 4c) can be explained by considering that as the sintering temperature increases, average grain size increases, and grain boundaries decrease, leading to a softer magnetic phase, approaching the properties of the "bulk."

The results for LFMA measurements at 77 K for the same samples, Figs. 4d to 4f, in contrast, exhibit strong changes in shape. A careful analysis of such changes leads to the conclusions that a progressive evolution from the positive LFMA signal toward a negative LFMA signal takes place. At the highest sintering temperature (500 °C), it is clear that the LFMA signal has the opposite sign. To complete the scheme, we have taken some results from recent publications discussing LFMA on monodisperse and clustered nanoparticles of the same composition [11], Fig. 5. In this figure, we show LFMA measurements for the same temperatures. It appears that at room temperature the clustered sample shows a positive LFMA signal, Fig. 5a. At 77 K (Fig. 5c), however, in addition to the tendency to show a positive signal, there are two additional peaks, which can be considered as the tendency to invert the signal. For monodisperse NPs, at low temperatures as shown in Fig. 5d, a small positive signal appears, while at room temperature (see Fig. 5b), there is only a flat response.

In order to interpret these results, we recall some recent experiments in bulk ferrites of a very close composition. In these experiments, a continuous evolution from negative to positive LFMA signal is observed as a function of the measuring temperature between 150 and 240 K, as shown in Fig. 6. It well known that in this temperature range and for composition with $x > 0.5$ (in the formula $Ni_{1-x}Zn_xFe_2O_4$), there is a competition in superexchange interaction between the two kinds of magnetic sublattices in the spinel structure, i.e., the B (octahedral) and the A (tetrahedral) sublattices. For the whole temperature range, the main superexchange interaction is the A–O–B (O stands for oxygen). However, for low temperatures and Zn content higher than ∼0.5, the B–O–B interaction can be comparable to the A–O–B inter-

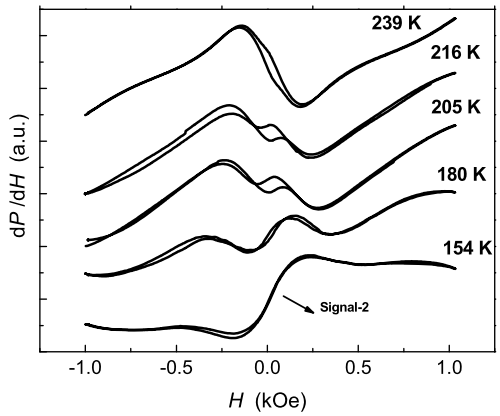

Fig. 6 Evolution of LFMA signal with temperature, in a bulk ferrite of the same composition (Ref. [10])

action, and a canted, or triangular spin arrangement occurs, first proposed by Yafet and Kittel [19].

In our case, the obtained results indicate that such Yafet–Kittel arrangement takes place only in the sample sintered at 500 °C; for lower sintering temperatures, there is the tendency but the LFMA signal is not fully negative. The LFMA observed in the monodisperse sample clearly shows a positive LFMA signal; for such small particles, no tendency to Yafet-Kittel structure appears. In a way, it seems that this spin arrangement has a cooperative nature and needs a larger volume to be established. The flat response at room temperature of monodisperse NPs is due to the fact that these NPs become superparamagnetic at a temperature well below 300 K [11]. This is an additional proof that LFMA is associated with magnetization processes in ordered ferro and ferrimagnetic phases.

4 Conclusions

Ni-Zn ferrite nanoparticles originally synthesized by the polyol method producing clusters were consolidated by the spark plasma sintering method (SPS) at temperatures in the 350–500 °C. The analysis of their low field microwave absorption, LFMA properties showed that the aggregation state is critical to form a Yafet–Kittel triangular (or canted) spin arrangement (YK), typically observed at low temperatures in bulk ferrites of Zn content ≥ 0.5. For monodisperse NPs of ∼6 nm, no evidence of YK structure was observed at 77 K. In these experiments, the Yafet–Kittel arrangement is associated with a negative LFMA signal. LFMA methods can become a powerful characterization technique.

Acknowledgements Authors thank A. Alvarez (IPN, Mexico) for microwave measurements. This work was partially supported by ANR (France)-CONACyT (Mexico) grant # 139292.

References

1. Medina, A.N., Knobel, M., Salem-Sugui, S., Gandra, F.G.: J. Appl. Phys. **79**, 5462 (2007)
2. Montiel, H., Álvarez, G., Betancourt, I., Zamorano, R., Valenzuela, R.: Appl. Phys. Lett. **86**, 072503 (2005)
3. Alvarez, G., Montiel, H., de Cos, D., Zamorano, R., Garcia-Arribas, A., Barandiaran, J.M., Valenzuela, R.: J. Non-Cryst. Solids **353**, 902 (2007)
4. Chiriac, H., Colesniuc, C.N., Ovari, T.-A., Ticusan, M.: J. Appl. Phys. **85**, 5453 (1999)
5. Chiriac, H., Colesniuc, C.N., Ovari, T.-A.: J. Magn. Magn. Mater. **215–216**, 407 (2000)
6. Montiel, H., Alvarez, G., Gutierrez, M.P., Zamorano, R., Valenzuela, R.: IEEE Trans. Magn. **41**, 3380 (2006)
7. Rivoire, M., Suran, G.: J. Appl. Phys. **78**, 1899 (1995)
8. de Cos, D., Garcia-Arribas, A., Alvarez, G., Montiel, H., Zamorano, R., Valenzuela, R.: Sens. Actuators A, Phys. **142**, 485 (2008)
9. Montiel, H., Alvarez, G., Gutierrez, M.P., Zamorano, R., Valenzuela, R.: J. Alloys Compd. **369**, 141 (2004)
10. Alvarez, G., Montiel, H., Barron, J.F., Gutierrez, M.P., Zamorano, R.: J. Magn. Magn. Mater. **322**, 348 (2010)
11. Valenzuela, R., Ammar, S., Herbst, F., Ortega-Zempoalteca, R.: Nanosci. Nanotechnol. Lett. **3**, 598 (2011)
12. Owens, F.J.: J. Phys. Chem. Solids **58**, 1311 (1997)
13. Srinivasu, V.V., Lofland, S.E., Baghat, S.M., Gosh, K., Tyagi, S.D.: J. Appl. Phys. **86**, 1067 (1999)
14. Gavi, H., Ngom, B.D., Beye, A.C., Strydom, A.M., Srinivasu, V.V., Chaker, M., Manyala, N.: J. Magn. Magn. Mater. **324**, 1172 (2012)
15. Beji, Z., Ben Chaabane, T., Smiri, L.S., Ammar, S., Fievet, F., Jouini, N., Greneche, J.M.: Phys. Status Solidi A **203**, 504–512 (1996)
16. Chkoundali, S., Ammar, S., Jouini, N., Fievet, F., Richard, M., Molinie, P., Villain, F., Greneche, J.M.: J. Phys., Condens. Matter **16**, 4357 (2004)
17. Munir, Z.A., Anselmi-Tamburini, U., Ohyanagi, M.: J. Mater. Sci. **41**, 763 (2006)
18. Orru, R., Lichen, R., Locci, A.M., Cao, G.: Mater. Sci. Eng., R Rep. **63**, 127 (2009)
19. Yafet, Y., Kittel, C.: Phys. Rev. **87**, 290 (1952)